

# Gain and noise characteristics of high-bit-rate silicon parametric amplifiers

Xinzhu Sang<sup>1,2</sup> and Ozdal Boyraz<sup>1\*</sup>

<sup>1</sup>Department of Electrical Engineering & Computer Science, University of California, Irvine, CA, 92697, USA

<sup>2</sup>Key Laboratory of Optical Communication and Lightwave Technologies (MOE), School of Electronic Engineering, Beijing University of Posts and Telecommunications, Beijing, 100876, China

\*Corresponding author: [oboyraz@uci.edu](mailto:oboyraz@uci.edu)

**Abstract:** We report a numerical investigation on parametric amplification of high-bit-rate signals and related noise figure inside silicon waveguides in the presence of two-photon absorption (TPA), TPA-induced free-carrier absorption, free-carrier-induced dispersion and linear loss. Different pump parameters are considered to achieve net gain and low noise figure. We show that the net gain can only be achieved in the anomalous dispersion regime at the high-repetition-rate, if short pulses are used. An evaluation of noise properties of parametric amplification in silicon waveguides is presented. By choosing pulsed pump in suitably designed silicon waveguides, parametric amplification can be a chip-scale solution in the high-speed optical communication and optical signal processing systems.

©2008 Optical Society of America

**OCIS codes:** (190.4380) Nonlinear optics; Four-wave mixing; (230.4320) Nonlinear optical devices; (250.3140) Integrated optoelectronic circuits; (250.4480) Optical amplifiers;

---

## References and links

1. G. T. Reed, "The optical age of silicon," *Nature* **427**, 595-596(2004).
2. C. Koos, L. Jacome, C. Poulton, J. Leuthold, and W. Freude, "Nonlinear silicon-on-insulator waveguides for all-optical signal processing," *Opt. Express* **15**, 5976-5990 (2007).
3. O. Boyraz and B. Jalali, "Demonstration of 11 dB fiber-to-fiber gain in a silicon waveguides," *Electron. Express* **1**, 429-434(2004).
4. A. Liu, H. Rong, R. Jones, O. Cohen, D. Hak and M. Paniccia, "Optical amplification and lasing by stimulated Raman scattering in silicon waveguides," *J. Lightwave Technol.* **24**, 1440-1445 (2006).
5. O. Boyraz and B. Jalali, "Demonstration of a silicon Raman laser," *Opt. Express* **12**, 5269-5273 (2004).
6. H. Rong, R. Jones, A. Liu, O. Cohen, D. Hak, A. Fang and M. Paniccia, "A continuous Raman silicon laser," *Nature* **433**, 725-728(2005).
7. X. Sang, E.-K. Tien, N.S. Yuksek, F. Qian, Q. Sang and O. Boyraz, "Dual-Wavelength Mode-Locked Fiber Laser with an Intracavity Silicon Waveguide," *IEEE Photon. Technol. Lett.* **20**, 1184-1186 (2008).
8. A. Liu, Jones, L. Liu, L. Liao et al, "A high speed silicon optical modulator based on a metal-oxide-semiconductor capacitor," *Nature* **427**, 615-618 (2004).
9. A. Liu, L. Liao, D. Rubin, H. Nguyen, B. Ciftcioglu, Y. Chetrit, N. Izhaky, and M. Paniccia, "High-speed optical modulation based on carrier depletion in a silicon waveguide," *Opt. Express* **15**, 660-668 (2007).
10. M. A. Foster, A. C. Turner, R. Salem, M. Lipson, and A. L. Gaeta, "Broad-band continuous-wave parametric wavelength conversion in silicon nanowaveguides," *Opt. Express* **15**, 12949-12958 (2007).
11. K. K. Tsia, S. Fathpour, and B. Jalali, "Energy harvesting in silicon wavelength converters," *Opt. Express* **14**, 12327-12333 (2006).
12. Y. -H. Kuo, H. Rong, V. Sih, S. Xu, M. Paniccia, and O. Cohen, "Demonstration of wavelength conversion at 40 Gb/s data rate in silicon waveguides," *Opt. Express* **14**, 11721-11726 (2006).
13. O. Boyraz, P. Koonath, V. Raghunathan, and B. Jalali, "All optical switching and continuum generation in silicon waveguides," *Opt. Express* **12**, 4094-4102 (2004).
14. V. R. Almeida, C. A. Barrios, R. R. Panepucci and M. Lipson, "All-optical control of light on a silicon chip," *Nature* **431**, 1081-1084 (2004).
15. V. R. Almeida, C. A. Barrios, R. R. Panepucci and M. Lipson et al, "All-optical switching on a silicon chip," *Opt. Lett.* **29**, 2867-2869(2005).
16. E. -K. Tien, N. S. Yuksek, F. Qian, and O. Boyraz, "Pulse compression and modelocking by using TPA in silicon waveguides," *Opt. Express* **15**, 6500-6506 (2007).
17. E. Tien, F. Qian, N. S. Yuksek and O. Boyraz, "Influence of nonlinear loss competition on pulse compression and nonlinear optics in silicon," *Appl. Phys. Lett.* **91**, art.201115 (2007).

18. R. Salem, M.A. Foster, and A.C. Turner et al, "Signal regeneration using low-power four-wave mixing on silicon chip," *Nat. Photonics* **2**, 35-38 (2008).
19. O. Boyraz, "Nanoscale signal regeneration," *Nat. Photonics* **2**, 12-13 (2008).
20. M. E. Marhic, K. K.-Y. Wong and L. G. Kazovsky, "Wide-band tuning of the gain spectra of one-pump fiber optical parametric amplifiers," *IEEE J. Sel. Top. Quantum Electron* **10**, 1133-1141(2004).
21. J. Hansryd, P. A. Andrekson, M. Westlund, J. Li, P.-O. Hedekvist, "Fiber-based optical parametric amplifiers and their applications," *IEEE J. Sel. Top. Quantum Electron* **8**, 506-520 (2002).
22. T. Torounidis and P. Andrekson, "Broadband single-pumped fiber-optic parametric amplifiers," *IEEE Photon. Technol.Lett.* **19**, 650-652 (2007).
23. T. Torounidis, P. Andrekson and B.-E. Olsson, "Fiber-optical parametric amplifier with 70-dB gain," *IEEE Photon. Technol. Lett.* **18**, 1194-1196 (2007).
24. M.-C. Ho, M. E. Marhic, Y. Akasaka and L. G. Kazovsky, "200-nm bandwidth fiber optical amplifier combining parametric and Raman gain," *J. Lightwave Technol.* **19**, 977-981 (2001).
25. K. K. Y. Wong, M. E. Marhic, G. Kalogerakis and L. G. Kazovsky, "Fiber optical parametric amplifier and wavelength converter with record 360 nm gain bandwidth and 50 dB signal gain," in *Conf. Lasers and Electro-optics 2003*, Baltimore, MD, Postdeadline paper CThPDB6.
26. H. Fukuda, K. Yamada, T. Shoji, M. Takahashi, T. Tsuchizawa, T. Watanabe, J. -i. Takahashi, and S. -i. Itabashi, "Four-wave mixing in silicon wire waveguides," *Opt. Express* **13**, 4629-4637 (2005).
27. Q. Lin, J. Zhang, P. M. Fauchet, and G. P. Agrawal, "Ultrabroadband parametric generation and wavelength conversion in silicon waveguides," *Opt. Express* **14**, 4786-4799 (2006).
28. A. C. Turner, C. Manolatu, B. S. Schmidt, M. Lipson, M. A. Foster, J. E. Sharping, and A. L. Gaeta, "Tailored anomalous group-velocity dispersion in silicon channel waveguides," *Opt. Express* **14**, 4357-4362 (2006).
29. M. A. Foster, A. C. Turner, J. E. Sharping, B. S. Schmidt, M. Lipson and A. L. Gaeta, "Broad-band optical parametric gain on a silicon photonic chip," *Nature* **441**, 960-963 (2006).
30. D. Dimitropoulos, R. Jhaveri, R. Claps, J. C. S. Woo and B. Jalali, "Lifetime of photogenerated carriers in silicon-on-insulator rib waveguides," *Appl. Phys. Lett.* **86**, art.071115 (2005).
31. M. Forst, J. Niehusmann, T. Plotzing and J. Bolten et al, "High-speed all-optical switching in ion-implanted silicon-on-insulator microring resonators," *Opt. Lett.* **32**, 2046-2048 (2007).
32. R. Espinola, J. Dadap, R. Osgood, Jr., S. McNab, and Y. Vlasov, "Raman amplification in ultrasmall silicon-on-insulator wire waveguides," *Opt. Express* **12**, 3713-3718 (2004).
33. R. A. Soref and B. R. Bennett, "Electrooptical effects in silicon," *IEEE J. Quantum Electron.* **QE-23**, 123-129 (1987).
34. H. A. Haus, *Electromagnetic Noise and Optical Measurements* (Springer-Verlag, 2000) pp. 197-237.
35. D. Dimitropoulos, D. R. Solli, R. Claps, O. Boyraz and B. Jalali, "Noise figure of silicon Raman amplifiers," *J. Lightwave Technol.* **26**, 847-852 (2008).
36. H.A. Haus, "Linearity of optical amplifiers and the Tomonaga approximation," *J. Opt. Soc. Am. B* **18**, 1777-1779(2001).
37. H. A. Haus and J. A. Mullen, "Quantum noise in linear amplifiers," *Phys. Rev* **128**, 2407-2413 (1962).
38. P. Kylemark, P. O. hedekvist, H. Sunnerud, M. Karlsson, and P. A. Andrekson, "Noise characteristics of fiber optical parametric amplifiers," *J. Lightwave Technol.* **22**, 409-416 (2004).
39. N. A. Olsson, "Lightwave systems with optical amplifiers," *J. Lightwave Technol.* **7**, 1071-1082 (1989).
40. M. E. Marhic, G. K. Kalogerakis, K. K. Wong, and L. G. Kazovsky, "Pump-to-signal transfer of low-frequency intensity modulation in fiber optical parametric amplifier," *J. Lightwave Technol.* **23**, 1049-1056 (2005).
41. D. Dimitropoulos, S. Fathpour, and B. Jalali, "Limitations of active carrier removal in silicon Raman amplifiers and lasers," *Appl. Phys. Lett.* **87**, art.261108 (2005).
42. S. F. Preble, Q. Xu, B. S. Schmidt, and M. Lipson, "Ultrafast all-optical modulation on a silicon chip," *Opt. Lett.* **30**, 2891-2893 (2005).
43. Y. Liu and H. K. Tsang, "Time dependent density of free carriers generated by two photon absorption in silicon waveguides," *Appl. Phys. Lett.* **90**, art.211105 (2007).
44. Y. Liu and H. K. Tsang, "Nonlinear absorption and Raman gain in helium-ion-implanted silicon waveguides," *Opt. Lett.* **31**, 1714-1716 (2006).
45. G. Kalogerakis, K. Shimizu, M. E. Marchic, K. K.-Y. Wong, K. Uesaka, and L. G. Kazovsky, "High-repetition-rate pulsed-pump fiber OPA for amplification of communication signals," *J. Lightwave Technol.* **24**, 3021-3027 (2006).

## 1. Introduction

The inherent lack of direct optical transitions makes silicon futile in photonic applications despite of its fame in microelectronic applications for over five decades [1]. However, recent developments in silicon based nonlinear optics fundamentally change this concept. The discovery of intrinsic high optical nonlinearity fortified by tight mode confinement and the

prospect of dense on-chip integration with micro- electronics make silicon photonics one of the rapidly growing research areas. A proper design of a silicon on insulator (SOI) based waveguide can deliver Kerr nonlinearity up to  $7 \times 10^6 \text{ W}^{-1} \cdot \text{km}^{-1}$  [2], which is more than three orders of magnitude larger than that of state-of-the-art highly nonlinear fibers, and facilitate chip scale nonlinear optical devices instead of long optical fibers. In fact, nonlinear photonic phenomena and devices in silicon, such as Raman amplification and lasing [3-7], optical modulation [8-9], wavelength conversion [10-12], all-optical switching [13-15], pulse compression [16-17] and optical signal regeneration [18-19] and so on, have been successfully demonstrated.

In particular, the demonstration of 6 dB/cm optical gain by Raman is attractive to optical communications [3]. However, in modern optical fiber communication systems, the dense wavelength division multiplexing (DWDM) with inline amplification is adopted to provide high capacity in a single fiber over a long distance. The relatively narrow Raman gain bandwidth of silicon can only amplify a few wavelength channels with one pump laser. Alternatively, optical parametric amplifiers (OPAs) through four-wave-mixing (FWM) can deliver large and flexible gain bandwidth [20-22]. OPAs and their applications are mainly demonstrated in highly nonlinear fibers of several hundreds meters. Fiber OPAs with single-stage gain of 70 dB [23] or gain spectra over more than 200 nm [24-25] have been realized. FWM in micrometer size silicon waveguides has been used for wavelength conversion, but it isn't suitable for parametric amplification due to low FWM efficiency operating in normal dispersion regimes [10, 26]. With a suitable small core waveguide design to shift zero dispersion wavelength toward the 1550 nm band, theoretical investigation shows that it is difficult to achieve net signal gain with a continuous-wave (CW) pump due to presence of two photon absorption (TPA) and free-carrier absorption (FCA) induced by TPA [27]. Recently, by tailoring the cross-sectional size and shape, the waveguide geometries that allow anomalous group velocity dispersion (GVD) have been investigated [28], and parametric amplification over 28 nm using a pulsed pump with a 75 MHz repetition rate has been demonstrated in suitably designed silicon waveguides [29]. However, net gain parametric amplification based on silicon is still a challenge under the presence of nonlinear losses, especially for high-speed optical communication and optical signal processing systems.

In this paper, we investigate the pumping conditions to achieve net gain and estimate the noise performance of silicon based parametric amplifiers in the presence of nonlinear losses at high bit rates. In particular, a detailed numerical investigation of the parametric gain and noise figure (NF) evolutions inside 1 cm silicon waveguides for high-repetition-rates are considered with waveguide parameters achieved experimentally [28-29, 30-32]. We show that for high data rates, net gain parametric amplification can be achieved by using shorter than 5ps pulses in anomalous dispersion regime. NF of the amplifier is influenced by the presence of nonlinear losses. In order to achieve net gain with a continuous-wave (CW) pump, the free carrier lifetime should be shorter than 20 ps. This paper is outlined as the following: In Section 2, we present the model used of the OPA in the silicon waveguide. Also, we present the NF evaluation method in the same section. In Section 3, we study gain profiles at different silicon GVD values and demonstrate the impact of peak pump power on parametric gain and NF at different wavelengths. The maximum gain, corresponding wavelength and NF are also discussed. The impact of pump pulse width and repetition rate on the parametric gain and NF is examined and compared. In the last part of this Section, we present the impact of different free carrier lifetimes on the parametric gain and NF, and the CW pumped OPA in silicon is discussed. Finally, in Section 4 we give a summary of our work.

## 2. Theory

### 2.1 Basic principles of OPA based on silicon waveguides

By combing a strong pump wave at angular frequency ( $\omega_p$ ) with a signal wave at another frequency ( $\omega_s$ ) into a silicon waveguide, FWM parametric process can occur. This can result in amplification of the signal as well as generation of an idler wave ( $\omega_i$ ) at the frequency

$\omega_i=2\omega_p-\omega_s$  at the same time. The evolution process of the pump  $A_p$ , signal  $A_s$  and idler  $A_i$  field amplitudes along the silicon waveguide can be described by the following coupled equations [11,27] assuming that  $|A_p| \gg |A_s| \gg |A_i|$

$$\frac{dA_p}{dz} = -\frac{1}{2}[\alpha + \alpha_p^{FCA}(z)]A_p + i\left(\gamma_p + i\frac{\beta}{2}\right)|A_p|^2 A_p, \quad (1)$$

$$\frac{dA_s}{dz} = -\frac{1}{2}[\alpha + \alpha_s^{FCA}(z)]A_s + 2i\left(\gamma_s + i\frac{\beta}{2}\right)|A_p|^2 A_s + i\gamma_s A_p^2 A_i^* \exp(-i\Delta k \cdot z), \quad (2)$$

$$\frac{dA_i^*}{dz} = -\frac{1}{2}[\alpha + \alpha_i^{FCA}(z)]A_i^* - 2i\left(\gamma_i - i\frac{\beta}{2}\right)|A_p|^2 A_i^* - i\gamma_i A_p^{*2} A_s \exp(i\Delta k \cdot z), \quad (3)$$

The first term on the right-hand side of Eqs. (1)-(3) is responsible for attenuations due to linear absorption and free-carrier absorption, the second term is responsible for SPM and TPA in Eq. (1) and XPM and TPA in Eqs. (2) and (3), and the last term in Eqs. (2) and (3) describes for the energy transfer between the interacting waves. We use the linear loss coefficient  $\alpha=1.4$  dB/cm, the TPA coefficient  $\beta=0.75 \times 10^{-11}$  m/W, and the nonlinearity coefficient  $\gamma_j=n_2\omega_j/c$  with the nonlinear refractive index  $n_2=5.5 \times 10^{-18}$  m<sup>2</sup>/W ( $j=p,s,i$ ).  $\Delta k$  is the phase mismatch due to propagation constants. The TPA-induced FCA loss is given as  $\alpha_j^{FCA}(z)=1.45 \times 10^{-17}(\lambda_j/1550)^2 N$ , where  $\lambda_j$  is the wavelength (nm),  $N$  (cm<sup>-3</sup>) is carrier density generated by TPA. Here  $N$  should satisfy the following rate equation at any position of the waveguide at any time [13]

$$\frac{dN(t,z)}{dt} = \frac{\beta}{2h\nu} I^2(t,z) - \frac{N(t,z)}{\tau} \quad (4)$$

In this equation,  $I_0$  is the peak intensity,  $h\nu$  is the photon energy and  $\tau$  is the effective carrier lifetime, which changes with the waveguide geometry or reverse bias voltage if a p-i-n diode structure exists. For CW pumping or long pulse pumping,  $N$  will reach the local steady state value of  $N(z) = \tau\beta I^2(z)/h\nu$ . For pulse pumping, the repetition rate  $R$  of the pulsed pump is an important factor impacting  $N$ . Under the operating condition of pulse pumping with pulse width  $T_0 \ll \tau$ ,  $N$  is given by

$$N(t,z) \approx \frac{\left(\frac{1}{1-e^{-1/R\tau}}\right)\beta T_0 I^2(t,z)}{2h\nu} \quad (5)$$

FWM is a coherent process whose efficiency depends on how well the phase mismatch  $\Delta k$  meets the phase-matching condition:

$$\Delta k = k_s + k_i - 2k_p + 2\gamma P_p = (n_s\omega_s + n_i\omega_i - 2n_p\omega_p)/c + 2\gamma P_p \approx \beta_2(\omega_s - \omega_p)^2 + 2\gamma P_p = 0 \quad (6)$$

where  $k_j$  is the propagation constant,  $\beta_2$  is the group velocity parameter. As the nonlinear part of the phase match is positive, phase matching can be realized by locating the pump wave in the anomalous dispersion regime ( $\beta_2 < 0$ ) so that the linear phase mismatch can compensate the nonlinear one. At the telecommunication wavelength of 1550 nm, the material dispersion of crystalline silicon is normal ( $D=-2\pi c\beta_2/\lambda^2=-880$  ps/(nm·km)). Because of the strong modal confinement in silicon waveguides, the waveguide dispersion can counteract the effect of the normal material dispersion [28]. It is experimentally verified that through proper design of waveguide shape and size, anomalous GVD in the range of 200-1200 ps/(nm·km) can be obtained at 1550 nm.

In addition to waveguide geometry and material dispersion, the TPA-induced free carrier dispersion (FCD) may also influence the phase-matching condition by changing the refractive index locally. Due to the free carrier plasma effect, the refractive index of silicon decreases linearly with increasing carrier density. However, the quadratic wavelength dependence of the free carrier plasma effect [33]

$$\Delta n_{FC} = -\frac{e^2 \lambda^2}{8\pi^2 c^2 \epsilon_0 n} \left( \frac{\Delta N_e}{m_{ce}^*} + \frac{\Delta N_h}{m_{ch}^*} \right) \approx -8.2 \times 10^{-22} \lambda^2 N \quad (7)$$

will alter the local dispersion and phase mismatching conditions as described in the following FCD equation:

$$\Delta D_{FC} = \frac{1}{c} \frac{d\Delta n_{FC}}{d\lambda} = -5.46 \times 10^{-30} \lambda N \quad (8)$$

Fig. 1(a) illustrates the FCD at 1550 nm based on the above analysis, when 5 ps pump pulses enter a 1 cm silicon waveguide with 300 ps free carrier lifetime and  $0.1 \mu\text{m}^2$  effective area. At low peak pump power and low repetition rate, the FCD value is small. Hence, when the repetition rate of the pulsed pump is low and the pulse width is short ( $< 2$  ps), the TPA-induced free carrier dispersion can be neglected. However, with increasing the repetition rate and the pulse width, FCD should be taken into the account, in particular at the input end of the silicon waveguides. The effect of the repetition rate plays an important role as the peak pump power is increased. For the relatively high peak pump power, the FCD can reach up to  $-300$  ps/(nm·km) if the repetition rate higher than 20 GHz. We should emphasize the fact that the FCD and FCA loss changes along the silicon waveguide due to attenuation of the pump pulses. As a result, the FCD may not be significant over long distances as illustrated in Fig. 1(b).

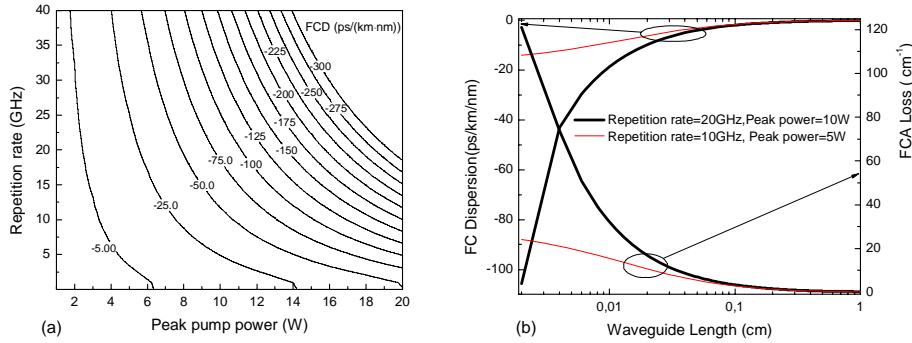


Fig. 1. (a). FCD contour as a function of peak pump and repetition rate at the input end. (b) FCD and FCA loss evolution along the waveguide

## 1.2 Noise properties

In an optical amplifier, the noise is induced by gain and loss fluctuations in the media [34-35]. For OPAs in silicon waveguides, the gain is generated by FWM process and the attenuation includes nonlinear losses of TPA, FCA and linear loss. The noise is analyzed by the Langevin noise sources, which are associated with photon fluctuation created by the gain and the loss in the optical amplifier [34-37]. This noise model can be extended to any linear optical amplifier. Main difference will arise from different loss components presented at different media. Since the nonlinear losses are absent in fiber OPAs, the analysis of noise in silicon OPAs is more complicated than that of fiber OPAs due to presence of nonlinear loss components. A detailed derivation of the noise calculation can be found in [34-35]. Here, noise induced by FWM process and contributions from other components are considered to estimate the final NF of an exemplary system presented in Fig. 2.

To estimate the NF due to FWM process, mean output photon number and mean photon number fluctuations through the silicon waveguide are calculated by using the signal wave Eqs. (1)-(3) [34-35]. The NF due to parametric amplification based on photon fluctuations will be:

$$NF_{silicon} = \frac{T + N_{loss} + N_{gain}}{T} + \frac{N_{gain}(T + N_{loss})}{T^2 |a|^2}, \quad (9a)$$

where

$$T = \exp\left(\int_0^L (g(z) - l(z)) dz\right), \quad (9b)$$

is the net gain and

$$N_{gain} = \int_0^L g(z) \exp\left(\int_z^L (g(x) - l(x)) dx\right) dz, \quad (9c)$$

$$N_{loss} = \int_0^L l(z) \exp\left(\int_z^L (g(x) - l(x)) dx\right) dz, \quad (9d)$$

are photon fluctuations due to gain and loss. Parameter  $L$  is the waveguide length,  $g(z)$  is the gain parameter that can be numerically calculated from Eqs. (1)-(3),  $l(z) = \alpha + \alpha^{FCA}(z) + 2\beta l(z)$  is the experienced loss coefficient,  $|a|^2$  is the photon number at the input frequency. Assuming that the input signal power is large enough, so the second term in Eq. (9a) is negligible and (9b)-(9d) can be numerically solved.

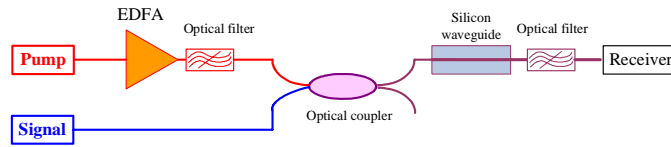


Fig. 2. Schematic configuration of the OPA in silicon waveguide

In order to achieve large pump power, optical pump sources around 1550 nm are often amplified with Erbium-dope fiber amplifier (EDFA), as illustrated in Fig. 2. The amplified spontaneous emission (ASE) of the EDFA together with the pump laser's relative intensity noise (RIN) influences OPA's noise performance and needs to be considered for final NF calculations. In general, the RIN is much less effective compared to ASE of the EDFA. Moreover, excess ASE of the amplifier outside the pump bandwidth,  $\Delta f$ , can be filtered before it is combined with the signal wave in the silicon waveguide. The variance of noise contribution on the pump due to the ASE of EDFA after the detections would be [38-39]

$$\sigma_{p-ASE}^2 = 4R^2 P_p S_{ASE} \Delta f \quad (10)$$

where  $S_{ASE} = n_{sp} h\nu (G_{EDFA} - 1)$  is the spectral density of ASE noise of the EDFA for amplifying pump laser,  $n_{sp}$  is the population inversion factor of EDFA set by 1.5,  $R = q/h\nu_s$  is the responsivity of the receiver. We know that larger the optical filter bandwidth will introduce more ASE noise. Therefore, an appropriate optical filter should be chosen for optimum noise performance. In addition, larger pump bandwidth is generally accompanied by pump relative intensity noise (RIN), which is magnified and transferred to Stokes and conjugate in OPAs and results in noise enhancement [40]. Here only the ASE contribution is included in our calculations and RIN transfer is excluded. The intensity variation of the noisy pump will result in signal gain variation because of its power dependence. The signal power variance caused by the noisy pump can be added as:

$$\sigma_{s-p}^2 = \sigma_{p-ASE}^2 \left( \frac{dG}{dP_p} P_s(0) \right)^2 \quad (11)$$

where the  $dG/dP_p$  value can be estimated by calculating the slope of the gain as a function of the pump power from Eqs. (1)-(3). The NF of amplified pump contribution to OPA can be given by [38]

$$NF_p = \frac{\sigma_{s-p}^2}{G^2 2R^2 h\nu P_s(0) \Delta f} = \frac{2P_p n_{sp} (G_{EDFA} - 1)}{G^2 P_s(0)} \left( \frac{dG}{dP_p} P_s(0) \right)^2 \quad (12)$$

So the total NF can be gotten by

$$NF = NF_{silicon} + NF_p \quad (13)$$

After the total noise sources are found, we can calculate the NF of OPA in the silicon waveguide by Eq. (13). In a 1 cm silicon waveguide operating in anomalous dispersion regime at 1550 nm, the typical gain and the linear NF spectra of the OPA pumped with 1 ps pulses operating at the repetition rate of 10 GHz are given in Fig. 3. As illustrated, the NF contribution from gain and loss fluctuations in the silicon waveguide is the dominant noise source of the silicon parametric amplifier.

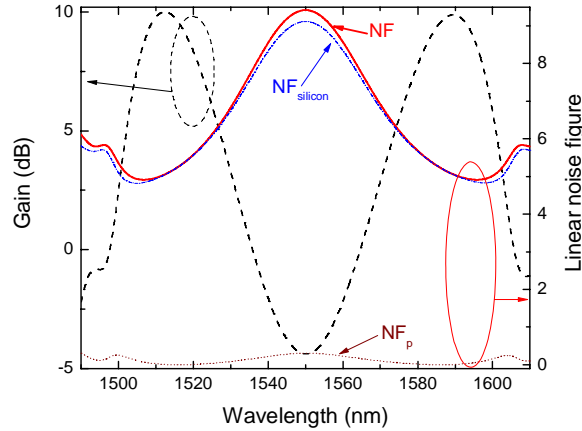


Fig. 3. Typical gain and NF spectra of OPA in the silicon waveguide

### 3. Results and discussion

To understand the gain and noise performances of OPA in silicon waveguides, we numerically investigate the impact of waveguide and pump pulse parameters based on related principles in Section II. The silicon waveguides have been considered to be 1 cm long with  $0.1 \mu\text{m}^2$  effective area. We should also realize that the gain and NF will scale with  $\tau R$ . In the following calculations of subsection 3.1-3.3, free carrier lifetime  $\tau$  of 300 ps is used to illustrate the performances achievable in those silicon nano-waveguides [28-29, 30-32]. In the last part, we discuss the impact of different free carrier lifetimes on the parametric gain and NF.

#### 3.1 Impact of the waveguide dispersion

To achieve net gain through parametric amplification, the pump wavelength should be operating in anomalous GVD regimes. To demonstrate this, 1 ps wide pump pulses centered at 1550 nm with 10 GHz repetition rate and 5 W peak power are used to investigate parametric gain at different dispersion values, and the results are summarized in Fig. 4. We clearly see that net gain can only be achieved within limited bandwidth in anomalous GVD regimes. The maximum gain achieved at the phase matching point shifts and the gain bandwidth decreases with increasing the dispersion value in the anomalous dispersion regimes.

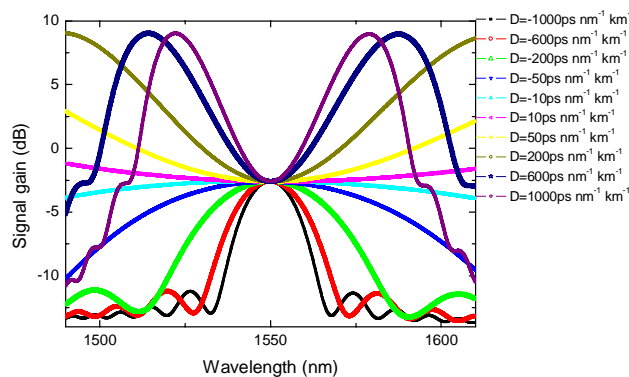


Fig. 4. Parametric gain profiles at different dispersion values.

### 3.2 Impact of Peak Pump Power

Pump power plays a significant role in OPA in silicon waveguides because TPA and FCA are both intensity-dependent. In addition, pump power also influence the local phase matching condition according to Eqs. (6) and (8). In the silicon waveguide with dispersion of 600 ps/(nm·km), 1 ps pulses at repetition rate of 10 GHz are used as pump. Signal gain and NF at eight wavelengths are investigated. With increasing the peak pump power, gain evolutions at eight wavelengths and maximum gain evolution are shown in Figs. 5(a) and 5(b), respectively. In Fig. 5(a), the gain decreases at relatively low peak pump power for some wavelengths which can be explained by nonlinear losses and phase mismatch. With increasing the peak pump power, the gain enters into saturation and then begins to decrease. The gain at the wavelengths near the pump wavelength enters into saturation earlier than that at the wavelengths far from the pump wavelength is due to shift of the phase matching point. The effects of phase matching by pump power are evident as the wavelength of maximum gain shifts significantly as depicted Fig. 5(b). We note that, unlike fiber OPAs, high peak pump power doesn't mean large gain due to presence of intensity-dependent TPA and FCA losses in the silicon waveguide, which is shown clearly in Figs. 5(a) and 5(b).

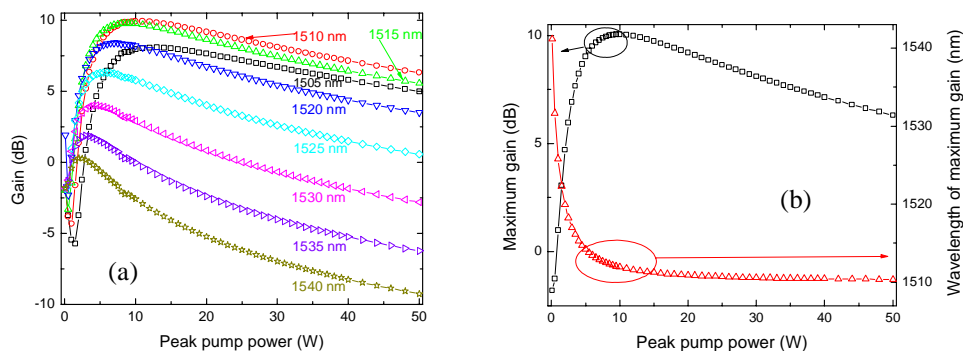


Fig. 5. (a). Gain evolution at different wavelengths, (b) Maximum gain and corresponding wavelength versus peak pump power.

In Fig. 6(a), the NF values are illustrated with respect to the peak pump power for eight different wavelengths. NFs increases with increasing the peak pump power, which is different from the gain evolutions. These results are expected because of the fact that the nonlinear



losses by TPA and FCA have significant contributions to the NF, from Eq. (9), and hence the NFs don't enter into saturation, as illustrated in Fig. 6(b).

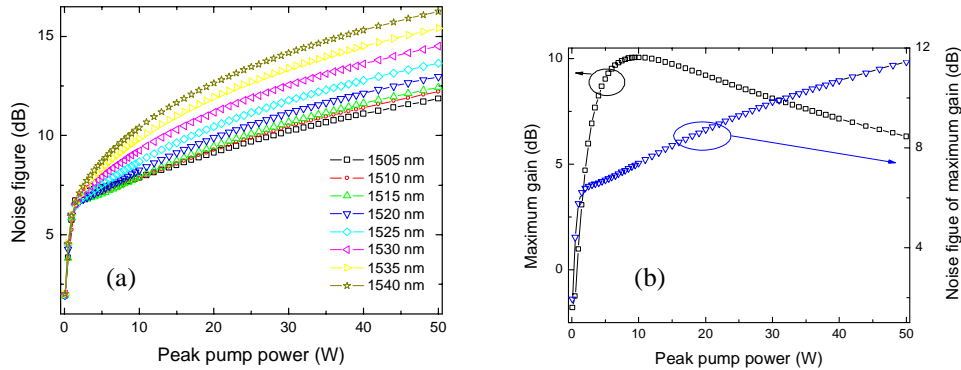


Fig. 6. (a). NF evolutions at different wavelengths. (b) NF evolution at maximum gain

### 3.3 Impact of pulse width and repetition rate of the pump

The repetition rate, and more importantly, pump pulse width have significant impact on parametric gain by influencing the free carrier density. Using pump pulses with peak power of 5 W and repetition rate of 10 GHz in the same waveguide as the above, parametric gain contour at different pulse width is shown in Fig. 7, in which the net gain regions are labeled by color. We can see that the net gain can only be achieved when the pulse width is below 5.2 ps and shorter pulse width can achieve wider gain bandwidth. Therefore, in order to achieve parametric gain in the silicon waveguide, short pulse mode-locked lasers should be considered. Shorter pulses mean higher gain that can be achieved.

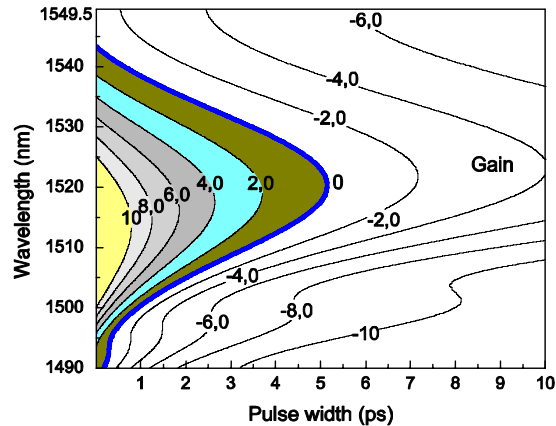


Fig. 7. Gain contour at different pulse widths

Fig. 8 shows the maximum gain and corresponding NF evolutions versus the repetition rate at four different pulse widths. We can know that the gain and NF have no significant changes when the repetition rate below 500 MHz, and the FCA loss is determined by the pulse width. With further increasing the repetition rate, the gain begins to decrease and the NF begins to increase, as displayed in Fig. 8(a). The net gain can even be achieved at 80 GHz when the pulse width is 0.5 ps, but there is no net gain for 10 ps at 5 GHz. The NF performances at different pulse width are illustrated in Fig. 8(b), which shows that lower NF can be achieved at shorter pulse and the NF increases with higher repetition rate when the repetition rate is above 1 GHz.

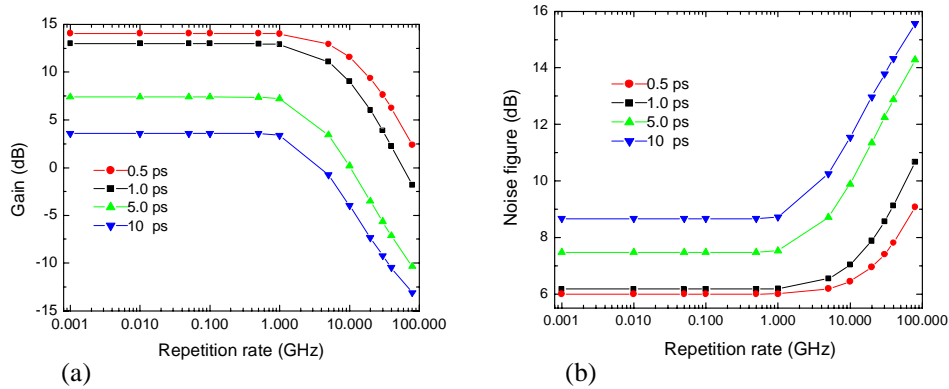


Fig. 8. (a). Parametric gain and (b). NF versus the repetition rate for different pulse widths

### 3.4 Impact of the free carrier lifetime

In the above analyses, we know that net gain and NF are strongly influenced by the free carrier loss and hence by the free carrier lifetime. The free carrier lifetime of 300 ps has been assumed to match the value which can be realized in passive silicon devices. Up to date, there are a few approaches presented to reduce the free carrier lifetime in silicon waveguides, which can be applied to these calculations. Active carrier removal by means of the electric field of a reverse-biased *p-n* junction is expected to reduce the free carrier lifetime to values close to 10 ps at low intensity excitation [6, 35, 41-42]. Additionally, ion implantation can be used to reduce the free carrier lifetime to 50 ps [31, 43-44].

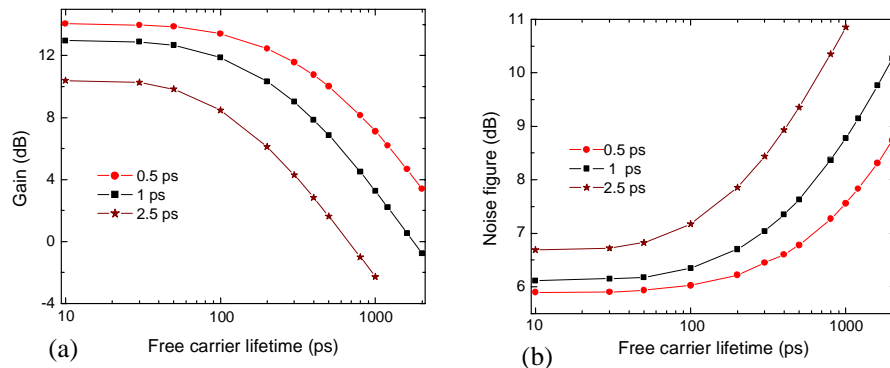


Fig. 9. (a). Parametric gain and (b). NF versus the free carrier lifetime for different pulse widths

To assess the effect of the free carrier lifetime, we calculate the optimum gain profiles and corresponding NF for free carrier lifetimes varying from 10 ps to 2000 ps, with pump pulse widths of 0.5 ps, 1 ps and 2.5 ps, as depicted in Fig. 9. We assume the repetition rate of 10 GHz and the peak pump power of 5 W. As illustrated, net gain can be achieved if the free carrier lifetime is below 500 ps with 2.5 ps pump pulses. To achieve net gain by a CW pump, the free carrier lifetime should be below 20 ps. For instance, Fig. 10 illustrates the optimum gain profile and the corresponding noise figure which can be achieved in a 1cm long silicon wire with free carrier lifetimes of 20 ps and 10 ps. Here, the optimum gains are achieved at peak pump powers of 4.6 W (4.6 GW/cm<sup>2</sup>) and 2.5 W (2.5 GW/cm<sup>2</sup>) for two free carrier lifetimes, respectively. As shown in these calculations the net parametric gain can be achieved at peak optical powers above 1W (1 GW/cm<sup>2</sup>). However, at these intensities, the generated free carriers will screen the applied electric field and null the lifetime reduction [41]. The

lifetime reduction by the ion implementation is achieved at the expense of the propagation loss and hence the induced linear loss might be prohibitive for these applications [31,43]. Although results presented in Fig. 9 and Fig. 10 assume that 1.4 dB/cm propagation loss can be maintained and the free carrier lifetime can be reduced simultaneously, these approximations may not hold in the real waveguide. Since, the dispersion value, the minimum free carrier lifetime and the parametric gain will be coupled, a further investigation is required to determine the optimum waveguide geometry for the CW pumped parametric amplification.

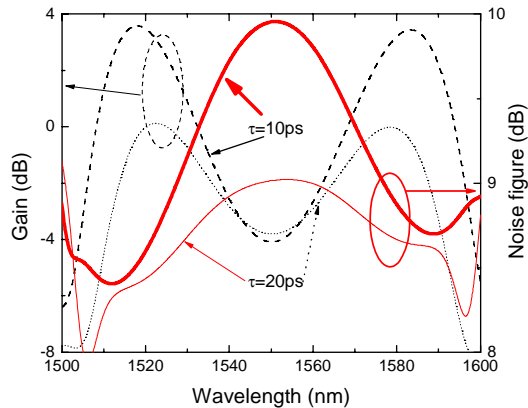


Fig. 10. Gain and NF spectra of OPA in the silicon waveguide with a CW pump.

#### 4. Conclusion

We investigate the gain and NF performances of the silicon based optical parametric amplifiers for high bit rate communication systems. In order to achieve net gain, the pump should operate in anomalous dispersion regimes and pump pulses should be  $<5$  ps for the free carrier lifetime of 300 ps. We show that the NF of the silicon parametric amplifiers increases due to nonlinear losses. Results indicate that for high bit rates, silicon based parametric amplification of WDM channels can be achieved by using pulsed-pump lasers, which are frequency and phase synchronized to all channels simultaneously. However, in real WDM systems high duty cycle modulation formats are being adapted and hence 5 ps pump pulses may not provide a good solution. Low duty cycle is adapted in the OTDM system, phase and frequency synchronizations are also a challenge for the high speed OTDM system with a pump laser. Recently the high-repetition-rate pulsed-pump OPA, followed by a narrowband optical filter, has been discussed for transparent signal amplification [45]. By choosing pulsed pump suitably designed for silicon waveguides, parametric amplification may be a chip scale solution in high-speed optical communications and optical signal processing systems.